Iraqi J. Laser, Part A, Vol.15, pp.25-34 (2016)

IRAQI JOURNAL OF LASER

Creating a Conductive Surface of the PMMA by Laser Cladding with DWCNT and MWCNTS

Wala I. Rasool and **Thaier A. Tawfiq**

Institute of laser for Postgraduate Studies, University of Baghdad, Baghdad, Iraq

(Received 3 October 2016; accepted 19 December 2016)

Abstract: This work studied the electrical and thermal surface conductivity enhancement of polymethylmethacrylate (PMMA) clouded by double-walled carbon nanotubes (DWCNTs) and multi-walled carbon nanotube (MWCNTs) by using pulsed Nd:YAG laser. Variable input factors are considered as the laser energy (or the relevant power), pulse duration and pulse repetition rate. Results indicated that the DWCNTs increased the PMMA's surface electrical conductivity from 10^{-15} S/m to 0.813×10^{3} S/m while the MWCNTs raised it to 0.14×10^{3} S/m. Hence, the DWCNTs achieved an increase of almost 6 times than that for the MWCNTs. Moreover, the former increased the thermal conductivity of the surface by 8 times and the later by 5 times.

Introduction

Modification of surface properties over multiple length scales plays an important role in optimizing material performance for a given application [1]. conductive polymer composites consisting of an insulating polymer matrix and a conductive filler, such as carbon black (CB), carbon nanotubes (CNTs) and carbon fibers (CFs) have attracted extensive attention in replacing metal parts in several applications including power electronic, electric motors and generators, heat exchangers, aerospace, military applications as a substitute for the high-strength fibers, in molecular wires, flexible electronics, electromagnetic induction shielding, electrostatic dissipation, and as biomolecule sensors [2]. Thanks to the polymer advantages such as light weight, corrosion resistance and ease of processing. Small loadings of MWCNT can enhance the electrical conductivity of polymeric composites up to several orders of magnitudes [3, 4]. Current interest to improve the thermal and electrical conductivities of polymers is focused on the selective addition of nanofillers with high thermal and electrical conductivities. This makes CNTs the best promising candidate material for conductive composites [5]. The first realized commercial application of CNTs in polymeric composites was for the purpose of electrical conductivity [6]. Ayub et al. [7] studied the electrical surface conductivity enhancement of injection-molded MWCNT/ PMMA nanocomposite by using CO_2 laser processing. They show that the irradiation of laser and utilization of covering gas could enhance the CNT–CNT contacts and the surface electrical conductivity. In addition, the conductive network generated from CNT–CNT contacts can transfer the electrical current. Annala [8] compared the electrical and mechanical properties of MWCNT/ polystyrene (PS) and MWCNT/PMMA nanocomposites produced by melt mixing and found that the electrical resistivity of the composites was more dependent on the method of CNTs addition. Lahelin M. et al. [9] investigated the mechanical and electrical properties of MWCNT/PS and PMMA. The results showed that the surface electrical resistivity was decreased by increasing amount of MWCNT. Wen-Tai H. and Nyan-Hwa T. [10] fabricated composites using CNTs as the reinforcement and PMMA as the matrix.

Their experimental results indicated enhancement of thermal conductivities over tenfold and near fifteen fold higher than PMMA for SWCNTs/PMMA and MWCNTs/PMMA composites, respectively. Villmow, T. et al. [11] showed that increasing the amount of MWCNT decreased the surface and volume resistivity of PMMA. Using CW lasers for cladding introduces too high heat input into the substrate for cladding slim and heat-sensitive components. The pulsed laser source is the one solution to this problem. Jensen [12] by using a pulsed Nd:YAG laser and conventional optics demonstrated the feasibility of using such a source for cladding applications.

The present paper is devoted to developing the conduction behavior of a well-known polymeric material by cladding its surface with two types of CNTs using pulsed Nd:YAG laser. The mathematical expressions associated with the pulsed laser are defined as follows [13];

$$E = t_P \times P_P$$

$$E = PRT \times P_{av}$$

$$PRT = PRR^{-1}$$

Where; E is the pulse energy, P_p is the peak power, P_{av} is the average power (W), *PRT* is the pulse repetition time (s), and *PRR* is the pulse repetition rate (Hz).

Materials and Work Setup

Poly-methyl-methacrylate (PMMA) of 2 mm in thickness supplied by Guanghe Huiji Co. Ltd./Beijing/China was chosen to be cladded by DWCNTs and MWCNTs using pulsed Nd:YAG laser. Both types of CNTs were supplied by Timesnano Company, Chengdu Organic Chemicals Co. Ltd., Chinese Academy of Sciences. The specifications of both CNTs types are shown in Table 1 according to the specification certificate issued by the previously mentioned companies. Table 2 illustrates both electrical and thermal properties of PMMA.

Table (1): Characteristics of the used CNTs.

Type	Diameter nm	Length μm	Purity wt%	Specific surface area m^2g^{-1}	Density g/cm^3	Thermal conductivity $Wm^{-1}K^{-1}$	Electrical conductivity Sm^{-1}
DW	2-4	~ 50	> 60	> 350	0.14	> 4000	$> 10^5$
MW	20-30	3-8	> 95	90-350	1-2	> 3000	10^6-10^7

Table (2): Characteristics of the used PMMA.

Characteristic	Amounts
Electrical resistivity	10^{14}-10^{15} Ω.cm
Surface resistance	10^{14} - 10^{16} Ω
Dielectric constant	2.8 - 4
CTE, linear 20°C	60 - 130 μm/m°C
Specific heat capacity	1.46 - 1.47 J/g°C
Thermal conductivity	0.19 - 0.24 W/mK
Maximum service temperature, air	41 - 103 °C
Melting point	130°C
Vicat softening point	47 - 117 °C
Glass temperature	100 - 105 °C

Figure 1 illustrates the employed work setup. The setup consisted of pulsed Nd:YAG laser of 1064nm, single pulse capability up to 70J/10 ms, pulse duration of 1-50 ms and frequency of 1-100 Hz. This apparatus was adapted to a manipulator through an optical fiber of 400 μm diameter.

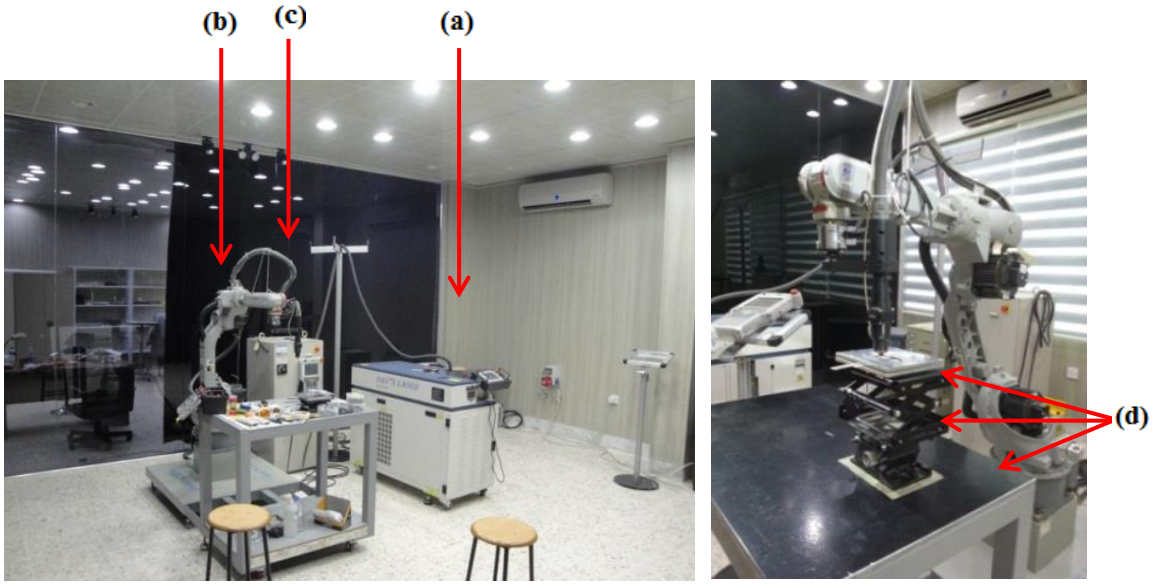

Fig. (1): Work setup; a) laser apparatus, b) manipulator, c) optical fiber, d) workstation.

All laser beam parameters including energy (the relevant peak power (P_p)), pulse duration (t_p) and frequency (PRR) were adjusted by the programmable logic controller (PLC) of the laser apparatus that is illustrated in Figure 2.

Fig. (2): Touch screen for parameter adjustment.

For each sample the pulse time was chosen in a manner that consists of two segments; 0.3 ms as preheating period and the rest as the main action time of the pulse. The employed manipulator was used to control the scanning speed and to achieve the precise positioning. The cladding process was accomplished using a line shaped spot of 9×0.5 mm in dimensions. The standoff distance between the tip of the laser head and the surface of the workpiece that achieved the minimum spot size was 86 mm. The scanning speed was fixed at 1 mm/s as a result of many trials to achieve better melting of the PMMA surface.

Experimental Procedure

Three groups, each one consisted of five workpieces were prepared to have the dimensions of 20 mm×20 mm×2 mm. The surfaces of all workpieces were cleaned by ethanol. The workpieces of the first group were illuminated by the laser beam in the absence of the CNTs, using five levels of P_p and constant t_p and PRR. All the workpieces of this group were tested using an optical microscope type OLYMPUS BX51/DP72 to distinguish the workpiece that had the best surface topography and that was clear of cracks, voids and discontinuity in the very first molten thin layer of its surface after processing. The work parameters of this workpiece were fixed for the next step. The same procedure was followed for the workpieces of the 2nd and 3rd groups. The 2nd group was processed using five levels of t_p at the same best value of P_p which was obtained from the 1st group and using the same value of PRR that was chosen for the 1st group. The same procedure was repeated for the 3rd group while varying the PRR and fixing the rest of the parameters. At the end the best work parameters were preset and a new set of workpieces was prepared for the final step. The final step consisted of applying the two types of CNTs powders as a paste on the pieces by using the preplaced powder cladding method. That paste was prepared by mixing the CNTs powder with ethanol. After 24 hours (for letting the ethanol to evaporate) a dry powder layer was attained that

adhered to the base material before irradiated by the laser beam. Figure 3 shows a schematic diagram for the cladding step.

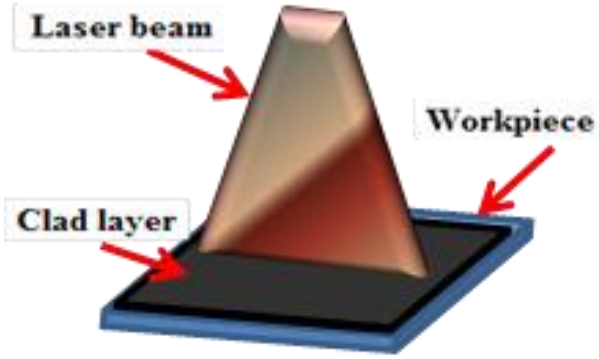

Fig.(3): Cladding process scheme.

Experimental Results and Discussion

Effect of Peak Power

Table 3 illustrates the preset work parameters for processing the 1st group showing the fifth workpiece as the best observed tested one by using the optical microscopic. Equation 1 illustrates that increasing the P_p for the same t_p and PRR increases the output E of the pulse as well. Moreover, increasing the P_p for the same projection area (4.5 mm^2) consequently increases the applied power density and subsequently increases the total amount of the applied thermal energy to the workpiece. Up to a certain limit of irradiance [14] this will enhance the quality of the cladding process. Above this limit the irradiance will be high enough to vaporize the material which will be detrimental to the process.

Table (3): Work parameters of the 1st group at t_p of 2.3ms and freq. of 10Hz

Group No.	Workpiece No.	P_p kW	P_{ave} W	E J	Power Density W/cm^2
G1	1	0.3	6.90	0.69	0.667×10^4
	2	0.4	9.20	0.92	0.889×10^4
	3	0.5	11.50	1.15	0.111×10^5
	4	0.6	13.80	1.38	0.133×10^5
	5	0.7	16.10	1.61	0.156×10^5

Effect of Pulse Duration

Table 4 illustrates the adjusted work parameters for the 2nd group showing the 3rd workpiece as the best observed tested one by using the optical microscopic. Equation 1 clarifies that increasing the t_p for the same P_p increases the output E of the pulse. Moreover, for the same PRR the overall amount of the applied thermal energy will be accumulated by increasing the t_p and leads to decrease the quality of the process by affecting the basic properties of the base material.

Table (4): Work parameters of the 2nd group at Pp of 0.7kW and P.R.R of 10Hz

Group No.	Workpiece No.	t_p ms	P_{ave} W	E J	Power Density W/cm^2
G2	1	1.3	9.10	0.91	0.156×10^5
	2	1.8	12.60	1.26	0.156×10^5
	3	2.3	16.10	1.61	0.156×10^5
	4	2.8	19.60	1.96	0.156×10^5
	5	3.3	23.10	2.31	0.156×10^5

Effect of Frequency

Table 5 illustrates the adjusted work parameters for the 3rd group showing the 4th workpiece as the best observed tested one by using the optical microscopic. Equation 1 shows that E is constant by keeping t_p and P_p constants. Therefore, increasing the PRR for the same scanning speed consequently increases the overlap between the laser pulses on the material's surface with decreasing the PRT and leading to increase the overall amount of the applied thermal energy per unit time.

Table (5): Work parameters of the 3rd group at Pp of 0.7kW and t_p of 2.3ms.

Group No.	Workpiece No.	Freq. Hz	P_{ave} W	Power Density W/cm^2
G3	1	8	12.88	0.156×10^5
	2	9	14.49	0.156×10^5
	3	10	16.10	0.156×10^5
	4	11	17.70	0.156×10^5
	5	12	19.32	0.156×10^5

Out of the whole workpieces of all groups, the workpiece G3/4 was found as the best observed one which had the best quality of the very first thin molten surface layer and best continuity of the clad material on the surface. Figure 4 shows the surface microscopic images of G1/5, G2/3, and G3/4.

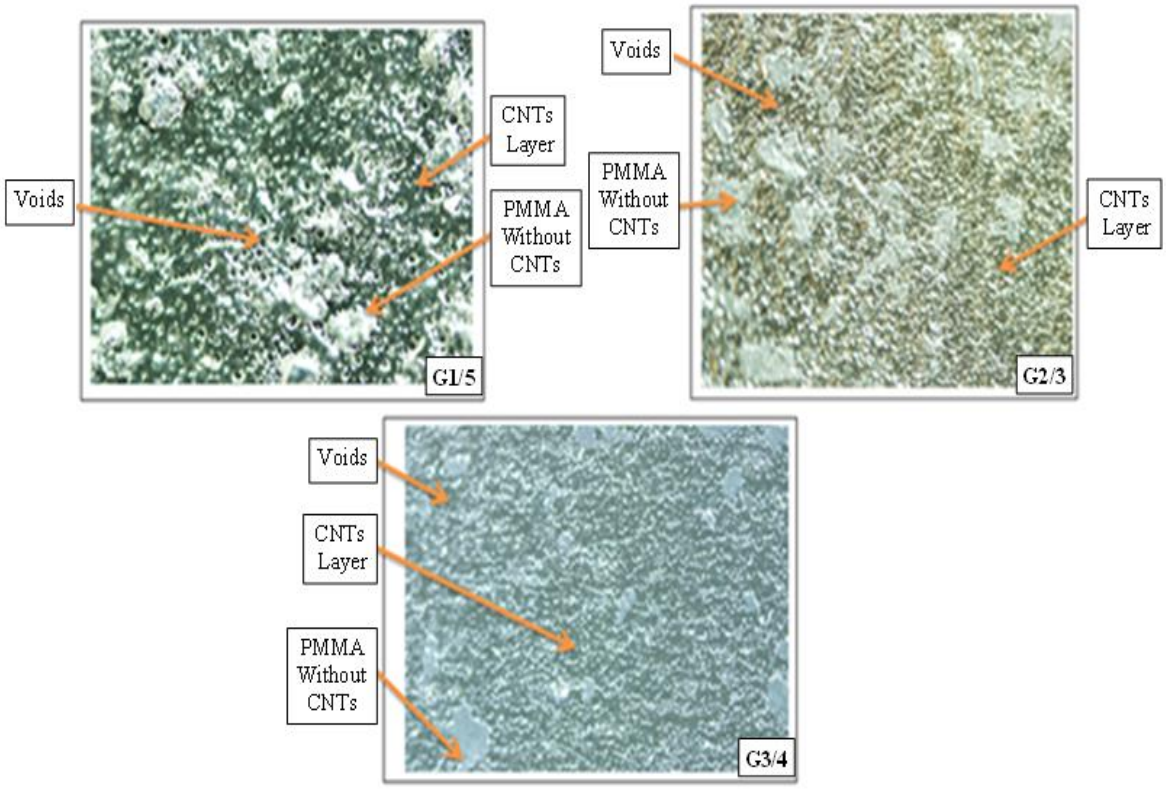

Fig. (4): Microscopic images of the best workpieces.

Energy-Dispersive X-Ray Spectroscopy (EDS or EDX) Test

This test covered the surface elemental analysis of each workpiece cladded by different type of CNTs. This test was designed to demonstrate the presence of highly concentrated CNTs on the PMMA surface after the cladding process. The workpieces cladded by both types of CNTs are shown in Figures 5 and 6. Table 6 shows the quantitative results and illustrates that the DWCNTs clad layer covered almost the whole surface of PMMA substrate better than that of the MWCNTs.

Table (6): Quantitative results of the workpieces cladded by both types of CNTs.

Elements	*wt% for PMMA Cladded by MWCNTs*	*wt% for PMMA Cladded by DWCNTs*	*at% for PMMA Cladded by MWCNTs*	*at% for PMMA Cladded by DWCNTs*
C	93.81	100.00	95.28	100.00
O	6.19	-	4.72	-

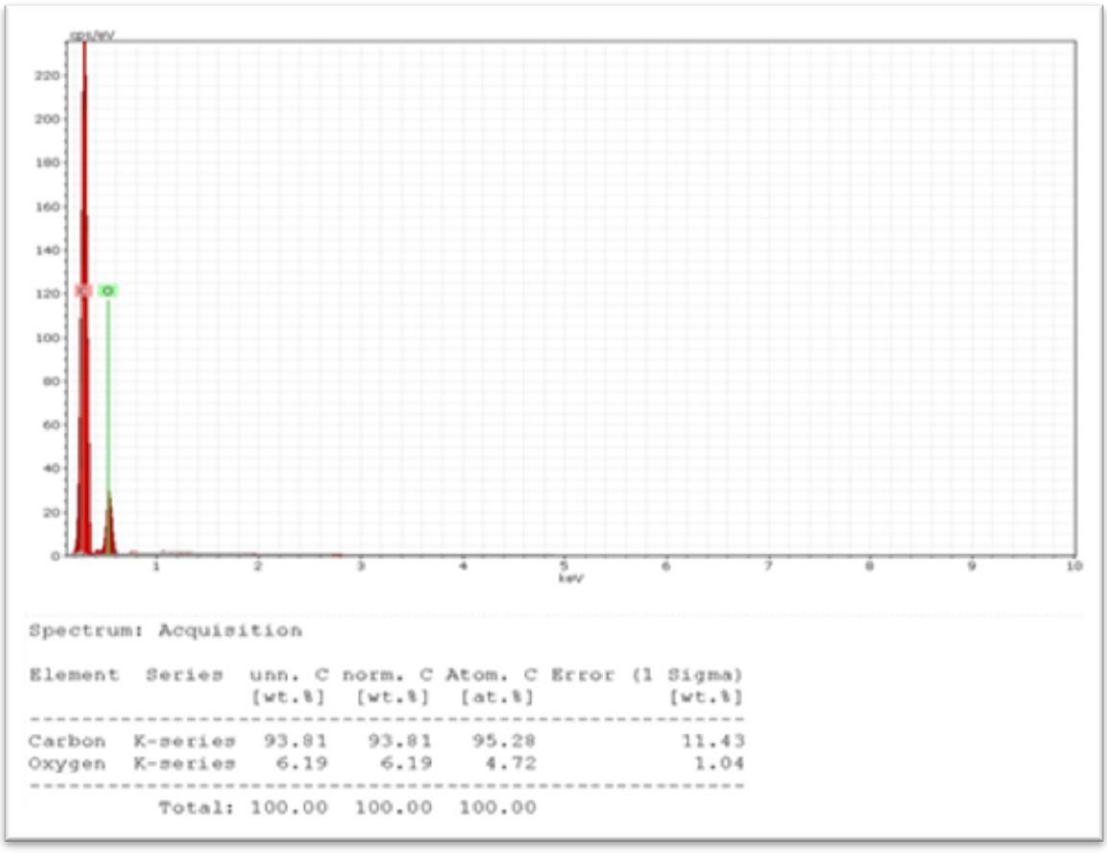

Fig. (5): EDS of the workpiece cladded by MWCNTs.

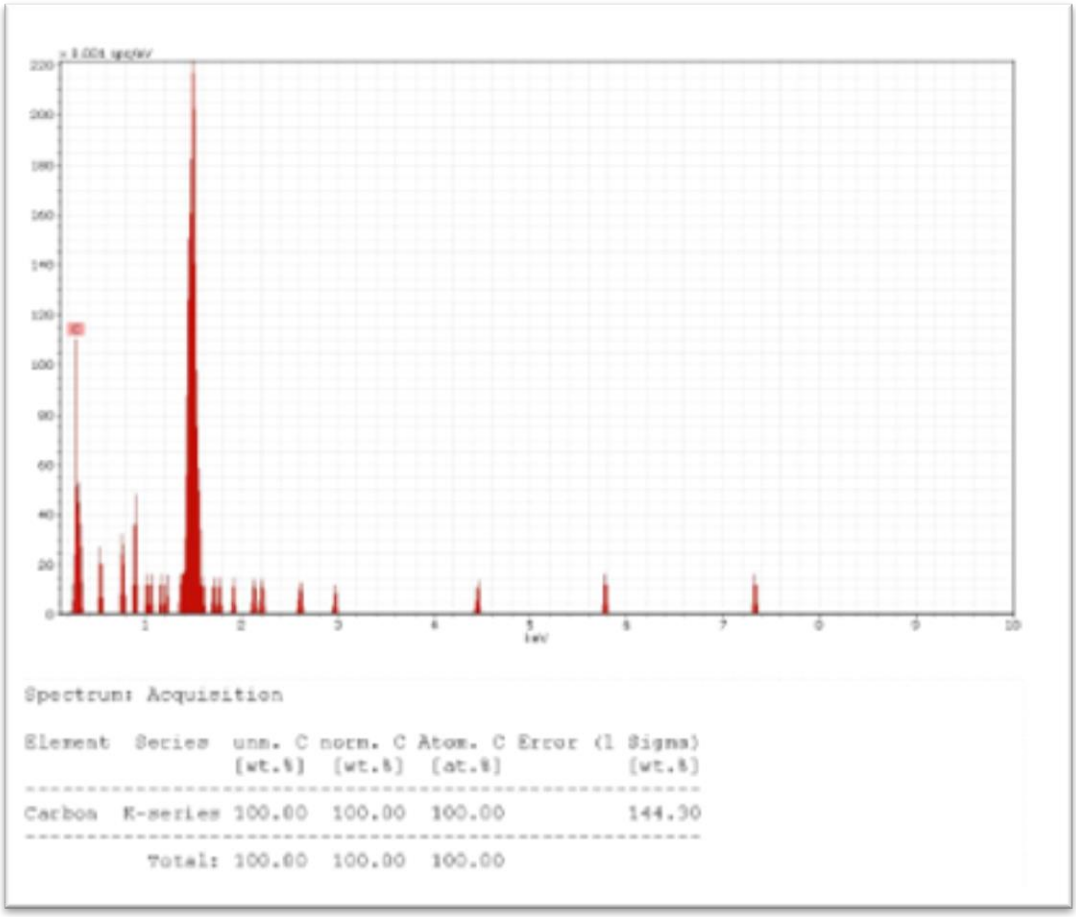

Fig. (6): EDS of the workpiece cladded by DWCNTs.

SEM Test

Figure 7 (a and b) illustrates the SEM images of the workpieces cladded by MWCNTs and DWCNTs respectively in order to distinguish which type of CNTs achieved better cohesion with the base material and to support the results which were obtained from the EDS test. These images demonstrated better distribution of the DWCNTs on the surface of the workpiece. Figure 8 shows the real observable images of the cladded workpieces.

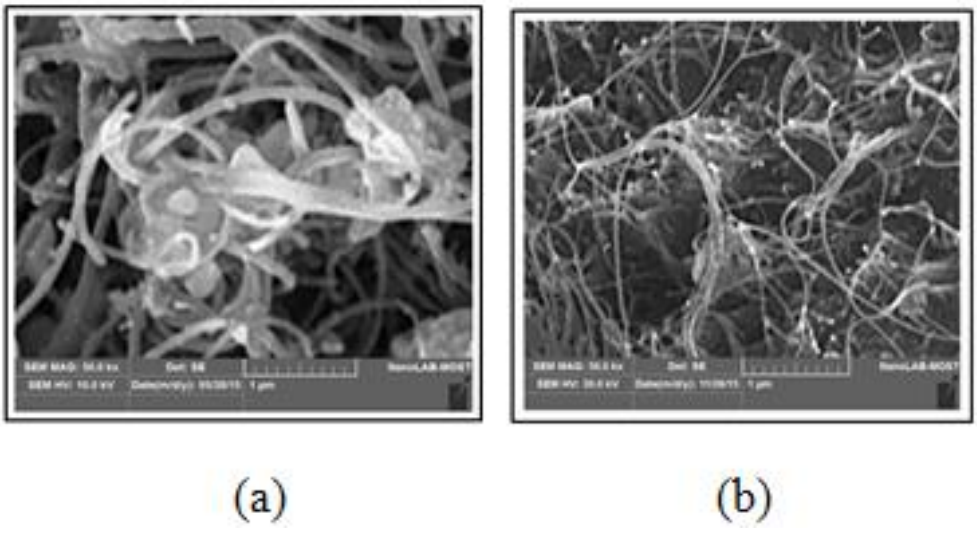

Fig. (7): SEM images; (a) workpiece cladded by MWCNTs. (b) workpiece cladded by DWCNTs.

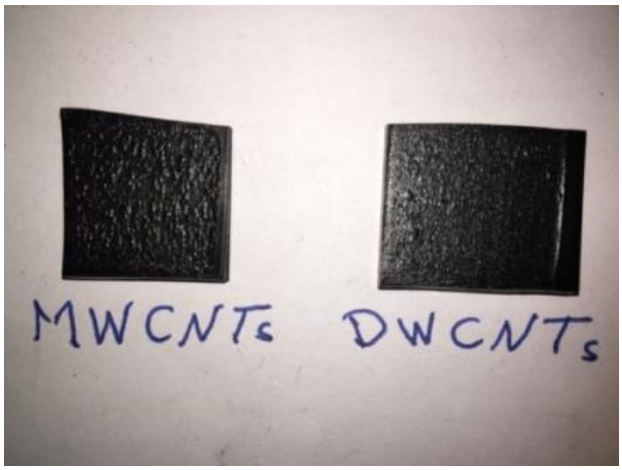

Fig.(8): Photos of the cladded workpieces.

Thermal Conductivity Test

This test measured the thermal conductivities of the workpieces cladded by both types of CNTs. It was achieved by using KD2 Pro thermal properties analyzer. These values then were compared with the thermal conductivity of the pure PMMA. For the benefit of this test, three workpieces cladded by MWCNTs and other three cladded by DWCNTs were produced using the same work variables. An average thermal conductivity value for each set of workpieces was estimated and compared with that of the pure PMMA as illustrated in Table 7.

Table (7): Thermal conductivities at 34.28 ºC.

Thermal conductivity of PMMA W/mK	***Thermal conductivity of workpiece Cladded by MWCNTs W/mK***	***Thermal conductivity of workpiece Cladded by DWCNTs W/mK***
0.19-0.24	1.203	1.713

Electrical Conductivity Test

A vacuum thermal evaporation system (speedvac unit) was used to measure the surface electrical conductivity of the cladded workpieces. By using this unit, a certain mask of pure aluminum was installed on the cladded workpieces in order to be used later on for measuring the electrical conductivity as shown in Figure 9.

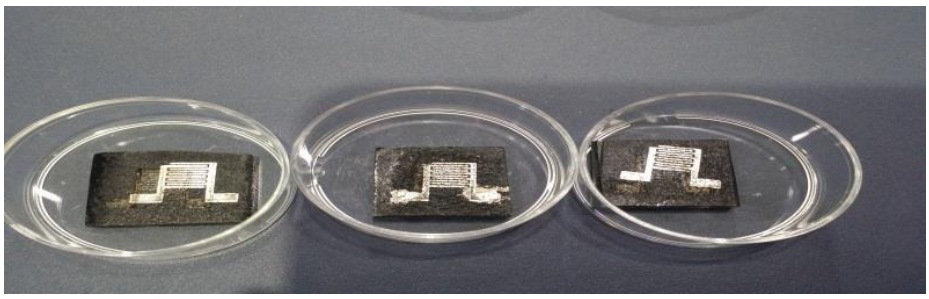

Fig. (9): Aluminum mask.

The recorded currents were plotted versus the applied voltages (V as the x-axis vs. I as the y-axis). The slope of the curve was then used in the following set of equations:

$V = IR$ ... ...(5)

$\rho = R\frac{A}{l}$ ... ... (6)

$\sigma = \frac{1}{\rho}$ ... ... (7)

Where:

V = voltage (V).

I = current (A).

R = electrical resistance (Ω).

ρ = electrical resistivity (Ω.m).

A = area of the mask (m^2).

L = length of the mask (m).

σ = electrical conductivity (S/m).

The average electrical conductivities of the three workpieces cladded by the; MWCNTs and DWCNTs were found to be; 0.14×10^3 S/m and 0.813×10^3 S/m respectively. Therefore, it is clear that both of these values are higher than that of the PMMA.

Table 8 shows the electrical conductivities for the workpieces cladded by the; MWCNTs and DWCNTs compared with the electrical conductivities of the pure PMMA and of the two types of CNTs.

Table (8): Electrical conductivities.

Electrical conductivity of PMMA S/m	***Electrical conductivity of MCNTs S/m***	***Electrical conductivity of DWCNTs S/m***	***Electrical conductivity of workpieces cladded by MWCNTs S/m***	***Electrical conductivity of workpieces cladded by DWCNTs S/m***
10^{-15}	10^6-10^7	$>10^5$	0.14×10^3	0.813×10^3

Conclusions

The results of this work showed the following;

1. Both types of CNTs achieved good distribution and homogeneity on the PMMA surface, but the DW type was the best.
2. Both types of CNTs changed the PMMA's surface status from being an insulator of 10^{-15} S/m electrical conductivity to a conductor of 0.813×10^3 S/m, by using the DWCNTs, and of 0.14×10^3 S/m when using the MWCNTs. Hence, the DWCNTs achieved an increase of almost 6 times than that for the MWCNTs.
3. The DWCNTs increased the thermal conductivity of the PMMA's surface by 8 times and the MWCNTs by 5 times than its original value.

References

1. J. Lawrence, D. J. Waugh, "Laser surface engineering: processes and applications", Elsevier, 2015.
2. Yamin Pan, Xianhu Liu, Xiaoqiong Hao, Zdeněk Starý, Dirk W. Schubert, " Enhancing the electrical conductivity of carbon black-filled immiscible polymer blends by tuning the morphology", Elsevier, European Polymer Journal ***78***, pp. 106–115, 2016.
3. Pötschke P., Bhattacharyya A. R., Janke A., Goering H., "Melt mixing of polycarbonate/multi-wall carbon nanotube composites", Journal Composite Interfaces, ***10***, 389, 2003.
4. Bryning M. B., Islam M. F., Kikkawa J. M., Yodh A. G., "Very low conductivity threshold in bulk isotropic single-walled carbon nanotube–epoxy composites", Advanced Materials, ***17***, 1186, 2005.
5. S. Berber, Y.K. Kwon, D. Tomanck, "Unusually high thermal conductivity of carbon nanotubes", Physical review letters, ***84***, 4613, 2000.
6. Baughman R. H., Zakhidov A. A., de Heer W. A., "Carbon nanotubes--the route toward applications", Science, ***297***, 787, 2002.
7. Ayub K. G., Taher A., Mohammadreza S., Amir N., Sina S., " Improving electrical conductivity of poly methyl methacrylate by utilization of carbon nanotube and CO_2 laser", Journal of Applied Polymer Science, 2015.
8. Annala M., "Utilization of polymethylmethacrylate carbon nanotube and polystyrene carbon nanotube in situ polymerized composites as masterbatches for melt mixing", Express Polymer Letters ***6***, 10, pp. 814–825, 2012.

9. Lahelin M., Annala M., Nykänen A., Ruokolainen J., Seppälä J, "In situ polymerized nanocomposites-Polystyrene/CNT and Polymethyl methacrylate / CNT composites", Elsevier, Composites Science and Technology, ***71***, 900, 2011.
10. Wen-Tai H., Nyan-Hwa T., "Investigations on the thermal conductivity of composites reinforced with carbon nanotubes", Elsevier, Diamond and Related Materials, ***17***, pp. 1577–1581, 2008.
11. Villmow T., Pegel S., Pötschke P., Wagenknecht U., "Influence of injection molding parameters on the electrical resistivity of polycarbonate filled with multi-walled carbon nanotubes", Elsevier, Composites Science and Technology, ***68***, pp. 777–789, 2008.
12. Jensen T. A., "Cladding of Hastelloy C on mild steel using a Nd:YAG laser", In: Proc. 2nd NOLAP Conference, Lulea, Sweden, Lulea University of Technology, pp. 9-24, 1989.
13. Y. F. Tzeng, "Pulsed Nd:YAG laser seam welding of zinc-coated steel", Welding Research Supplement, Department of Mechanical Engineering, Chang Gung University, Taiwan, 1999.
14. L. George, V. Wielligh, "Characterizing the influence of process variables in laser cladding Al-20WT% Si onto an Aluminium Substrate", Thesis (M.Tech.), Nelson Mandela Metropolitan University, 2008.

تكوين سطح موصل لبولي ميثيل ميثاكريلايت بالأكساء بالليزر مع انابيب كاربون نانوية ثنائية الجدران وانابيب كاربونية متعددة الجدران

ثائر عبد توفيق ولاء عصام رسول

معهد الليزر للدراسات العليا ، جامعة بغداد ، بغداد ، العراق

الخلاصة يتناول هذا البحث إكساء سطح بوليمر (بولي مثيل ميتاكريلات) بأنابيب كاربون نانوية، ثنائية ومتعددة الجدران، بإستخدام ليزر الياك النبضي لأنتاج بوليمر ذو خاصية مزدوجة للتوصيل الحراري والكهربائي. تم تحقيق هذا الهدف من خلال التحكم بطاقة نبضة الليزر، زمن النبضة، والتردد. دلت النتائج على إن كلا نوعي أنابيب الكاربون النانوية قد غيرت حالة الموصلية الكهربائية لسطح البوليمر (بولي مثيل ميتاكريلات) من كونه عازل كهربائي ذو قيمة موصلية كهربائية مقدارها 10^{-15} سيمنس/متر الى موصل كهربائي بقيمة موصلية كهربائية مقدارها 0.813×10^{3} سيمنس/متر عند الإكساء بأنابيب الكاربون النانوية مزدوجة الجدران، والى موصل كهربائي بقيمة موصلية كهربائية مقدارها 0.14×10^{3} سيمنس/متر عند الإكساء بأنابيب الكاربون النانوية متعددة الجدران. عليه فإن الإكساء بأنابيب الكاربون النانوية مزدوجة الجدران قد حسنت الموصلية الكهربائية بمقدار ست مرات أفضل مما حققته أنابيب الكاربون النانوية متعددة الجدران. كما إن أنابيب الكاربون النانوية مزدوجة الجدران حسنت الموصلية الحرارية للسطح بمقدار ثمان مرات عن القيمة الحقيقية للبوليمر بينما حققت أنابيب الكاربون النانوية متعددة الجدران زيادة في الموصلية الحرارية للسطح بمقدار خمس مرات عن القيمة الحقيقية للبوليمر.